Comparative study of luminescence and chemiluminescence in hydrodynamic cavitating flows and quantitative determination of hydroxyl radicals production

Lionel Perrin, Damien Colombet, Frédéric Ayela

Comparative study of luminescence and chemiluminescence in hydrodynamic cavitating flows and quantitative determination of hydroxyl radicals production.

L. Perrin, D. Colombet and F. Ayela[a].

Laboratoire des Ecoulements Géophysiques et Industriels, Univ. Grenoble Alpes, CNRS, 38000 Grenoble France.

Luminescence and chemiluminescence have been experimentally investigated in hydrodynamic cavitating flows. By using dedicated microdevices inserted inside a light tight box, photons counting has been made possible. Luminescence has been investigated with deionized water as the working fluid ; chemiluminescence has resulted from cavitating alkaline luminol solutions, and has been correlated to hydroxyl radicals formation. For the first time, luminescent and chemiluminescent phenomena have been considered together on the same devices submitted to similar cavitating flow regimes. Degassed solutions enhance the luminescence and also the hydroxyl radical yield. Due to the small sizes of the channels, the lifetimes of the collapsing bubbles correspond to pseudo frequencies matching the range of optimal frequencies used in sonochemistry. New perspectives for the study of hydrodynamic cavitation as an advanced oxidation process are suggested.

Keywords : Hydrodynamic cavitation, luminescence, chemiluminescence, radical production.

1. Introduction

Cavitation refers to the growth and violent collapse of vapor bubbles in a liquid. This phenomena encompasses various physical issues, such as fluid mechanics, thermodynamics, physics and chemistry. Tremendous effects are associated to cavitation, of which the emission of light is among the most striking. Sonoluminescence and chemiluminescence have been widely studied in acoustic cavitation, when bubbles are monitored by ultrasonic waves. Sonoluminescence depends on the size of the bubbles, on the intensity and on the frequency of the acoustic field, and on the amount of dissolved gases in the liquid. It has been demonstrated [1, 2] that a plasma forms in bubbles at collapse, and light is emited from non condensable species in excited states. Furthermore, water molecules splitting caused by the collapses can result in the formation of hydroxyl radicals $OH^{\bullet}$ and of hydrogen peroxide molecules, that is a part of sonochemistry. Luminol has been used in sonochemical and radiolysis experiments as a telltale product. Chemiluminescence in the liquid phase results then from chemical reactions of luminol molecules with hydroxyl $OH^{\bullet}$ and with superoxide O_2^- [3-9].

Sonoluminescence and sonochemistry result both from the collapse of bubbles, but the physical processes respectively involved are rather different. Sonoluminescence is enhanced in degassed liquids and in mixtures exhibiting a low vapour pressure, because polyatomic molecules such as H_2O, N_2, O_2 present inside the bubbles are likely to quench the collapse and to absorb some amount of energy. At first sight, low water vapour pressure conditions appear to be unfavourable to induce a high yield of hydroxyl radicals. More precisely, the shape and the size of the collapsing bubble is believed to be crucial [10]. Single bubble sonochemiluminescence experiments in aqueous luminol solutions have demonstrated that $OH^{\bullet}$ production and diffusion toward the liquid phase is made possible from unstable bubbbles, which do not emit sonoluminescence [6]. Hydroxyl radicals produced inside stable

[a] Corresponding author : frederic.ayela@legi.cnrs.fr

spherical bubbles, if any, are believed to be locked in the core of the plasma and to react with other components present in the plasma [2, 11].

Almost all the publications refering to luminescence, sonochemistry and chemiluminescence, consider only acoustic cavitation, which exerts on limited amounts of liquid submitted to ultrasonics waves. Another form of cavitation is hydrodynamic cavitation, that is the consequence of the Bernoulli law for liquid flows. A local constriction of the free flow area is accompanied by an increase of the average velocity, that can reduce the static pressure below the vapour pressure P_{vap} and incept a cavitating two phase flow. Downstream, where the flow area increases, the velocity falls down and the static pressure recovers a value above P_{vap}, so that bubbles and vapour clouds collapse. Hydrodynamic cavitation can develop either in turbulent shear layers downstream orifices and diaphragms, or in vapour sheet layers downstream the throat of a Venturi. Unlike acoustic cavitation where bubbles oscillations are monitored, bubbles dynamics in hydrodynamic cavitation is complex and the duration in which a liquid molecule is submitted to the cavitating two phase flow regime is rather short, even if large volumes of liquid can be considered. Maybe that is why luminescence in hydrodynamic cavitation is less attractive than single bubble or multi bubbles sonoluminescence, and that the rate of publications dealing with luminescence in hydrodynamic cavitating flows is limited to a few papers.

Jarman and Taylor [12, 13] detected luminescence that was associated to two phase cavitating tap water flows through a polypropylene Venturi tube. Light emission came from the region where vapour clouds and bubbles are likely to collapse. The intensity of such an hydroluminescence was claimed to be weaker than that of sonoluminescence, although a comparison of the corresponding emitting volumes was not presented. The emission of light was enhanced by the addition of carbon disulfide in water. The authors claimed that the emission of light was caused by high temperature inside the collapsing bubbles, and that CS_2 molecules, which were present inside, could be also sensitive to collapses that induce lower temperatures. The role of carbon disulfide was studied later by Didenko et al. [14]. They have observed that the addition of small amounts of CS_2 enhanced the acoustic multibubble sonoluminescence, whereas other organic liquids quenched the luminescence. It was stated that luminescence from water – CS_2 mixtures was emited by the fluorescence from excited states of CS_2 inside the collapsed bubble.

Using a quartz Venturi tube, Peterson and Anderson confirmed that light emission occured at the end of the collapsing region of the cavity [15]. By increasing water temperature, they observed that there was a decrease of the light intensity, that may be explained by the fact that the higher temperature, the higher vapour pressure and so the higher number of polyatomic water molecules able to quench the collapse. They recorded individual short light pulses and they noticed that the presence of dissolved Xe gas in water increased drastically the light intensity. The respective roles of Xe dissolved gas and of the temperature of the degassed water were confirmed by Weninger et al [16], who also used a quartz Venturi tube. The light enhancement caused by Xe, compared to other gases, was stronger in the ‘one shot’ hydrodynamic luminescence process than with sonoluminescence monitored by acoustically driven bubbles.

Leighton et al. [17] studied another form of hydrodynamic cavitation over an hydrofoil, and observed luminescence from undegassed water without any noble gas addition. The counted photons increased with the velocity of the fluid. Light emission was correlated to the shedding frequency of the attached cavity [18].

A recent paper has considered cavitating flow luminescence emitted downstream the submillimeter restriction of glass Venturi tubes [19]. Mixtures of deionized distilled water and dimethyl sulfoxide were considered at different temperatures, to scrutinize the role of vapour pressure on the quenching of the collapse of the bubbles. Noble gases were also sparged in

some mixtures. Although the signals recorded by a photomultiplier tube (PMT) seemed to only slightly emerge from the residual noise level, classical conclusions were confirmed. In low vapour pressure mixtures, quenching of the collapse of the bubble is reduced and the presence of rare gases molecules with low energy excitation levels enhances the luminescence. By using three Venturi with different restriction sizes, the authors could establish that the intensity of the luminescence does not depend on the absolute value of the flow rate, but on the total pressure drop.

Hydrodynamic luminescence is also considered as a possible consequence of the friction of a liquid on the walls of a narrow dielectric channel [20]. A non uniform distribution of electric charges on the bubbles walls may induce discharges in the vapour phase.

Chemistry induced by hydrodynamic cavitation [21] is significantly less studied than sonochemistry. On the one hand, hydrodynamic cavitation requires setup with larger volumes than ultrasonic reactors. On the other hand, it is believed that the weak luminescent level from hydrodynamic cavitation is correlated to a weak $OH^{\bullet}$ radicals production yield. Empirical research has been performed to test some chemical reactions [22 – 24]. In these experiments, the flow is driven by a centrifugal pump in which cavitation is also likely to occur [25], making a fine analysis of the role of hydrodynamic cavitation more complex. Cavitation-induced pyrolysis reactions have been recently suggested as the explanation of hydrodynamic luminescence in a Diesel injector valve [26]. A question remains, that is a direct evidence of the hydroxyl radical production yield downstream hydrodynamic cavitating reactors. As mentioned above, it is well known that solutions of luminol emit light when exposed to ultrasound [3 – 5]. Light results from chemical reactions between luminol and $OH^{\bullet}$ radicals produced within the bubbles [3]. Surprisingly, the first experimental demonstrations of the chemiluminescence of luminol solutions in hydrodynamic cavitating reactors are still very new [27, 28]. Schlender et al. [27] stated that the cavitation intensity was directly related to the hydroxyl radical formation. They characterized qualitatively luminol solutions through a high pressure double stage homogenization setup and they visualized chemiluminescence downstream submillimeter orifices. Podbevsek et al. [28] used transparent microdiaphragms feeded with luminol in a light tight box, and counted the emitted photons in a cavitating flow regime. In the range of flow rates considered, the number of photons increased linearly with the flow rate. No clear evidence of luminescence was detected when using water engassed with argon as the working fluid, but the maximum flow rates did not exceed 150 µl/s.

A better knowledge of the hydrodynamic cavitation phenomena can help the development of innovative wastewater treatments. Cavitation is among the smartest concept currently devoted to the remediation of wastewater by an advanced oxidation process [29, 30]. But hydrodynamic cavitation is more complex than ultrasonic cavitation, for which the frequency of excitation, the acoustic power and the duration of exposition can be clearly controled. Concerning hydrodynamic cavitation, the pressure drop and/or the average velocity of the fluid through the constriction can be monitored ; but the number of cycles of a bubble, its shape, and the influence of interbubble interactions on the cavitation intensity are out of the range of accessible data. We have attempted to compensate for the lack of experimental data, by performing a comparative study in which for the first time, both luminescence and chemiluminescence phenomena induced by a cavitating flow have been recorded and analysed. That has been made possible with hydrodynamic cavitation ‘on a chip’, that is cavitation inside transparent micromachined silicon – Pyrex reactors [31, 32]. Such devices, which require a low amount of fluid, produce a conventional two-phase cavitating flow and their small sizes make them convenient for experiments that require specific conditions unavailable at macroscale [33, 34]. So hydrodynamic cavitation ‘on a chip’ is well suited for experiments where external light must be prohibited. Preliminary attempts had successfully confirmed the formation of hydroxyl radicals in cavitating flows [28]. Here, we have used a

new design of microreactors and a new setup that have made possible, from the same device, the quantitative observation of both chemiluminescence of luminol and luminescence of deionized water.

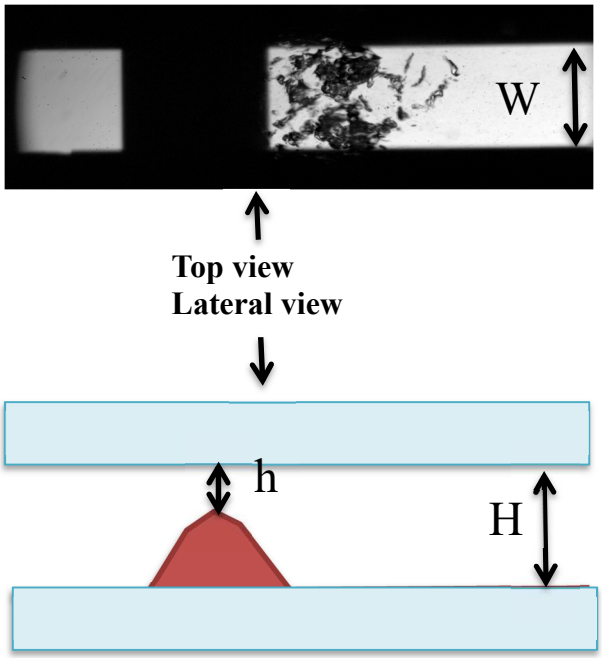

a)

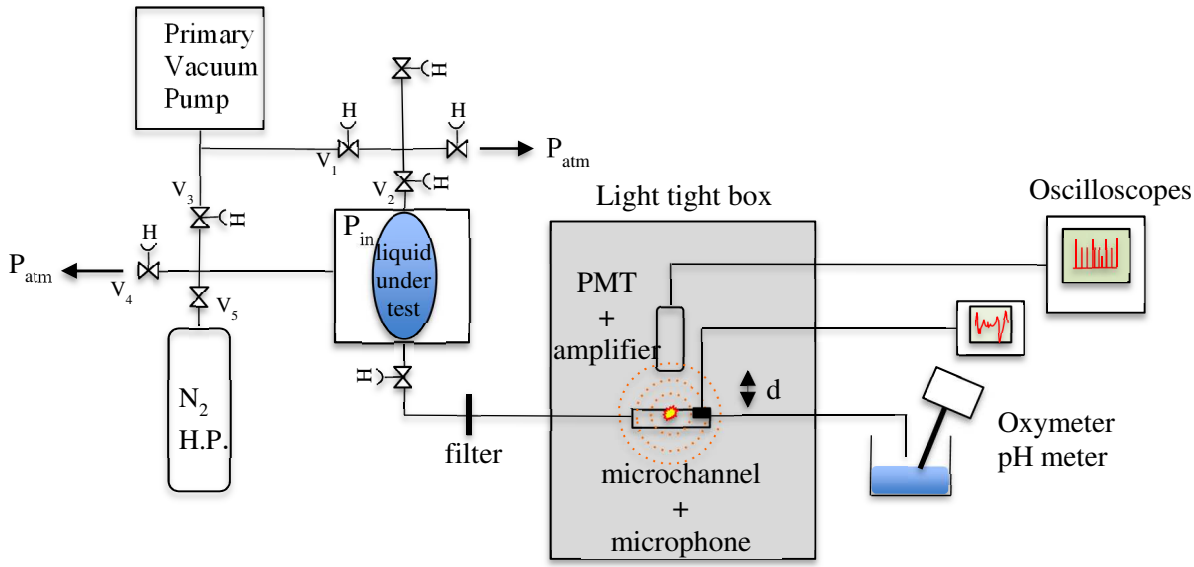

b)

Figure 1. a) *Views of a microstep cavitating device (not at scale) ;* b) *Experimental set up dedicated to luminescent and chemiluminescent measurements inside hydrodynamic cavitating microflows.*

2. Experimental set up

The key components of the experiments presented here are the microreactors in which hydrodynamic cavitation arises. They are hybrid silicon – Pyrex micromachined devices. Most of the experiments have been performed with a so-called microstep device (MSD). Complementary experiments have been performed with a so-called microdiaphragm device (MDD). The design and the microfabrication steps of such devices have been presented previously [31, 35]). Both are able to exhibit shear cavitation downstream a microstep situated perpendicularly to the flow (MSD) or downstream a rectangular microdiaphragm (MDD). The profiles are machined onto a silicon wafer, by KOH wet etching (MSD) or deep reactive ion etching (MDD). A transparent Pyrex drilled cap is then anodically bonded onto the silicon channel. Hydrodynamic cavitation 'on a chip' is possible only when it is the smallest size of the channel which is diverging [31]. In the microstep configuration, the height h of the gap between the top of the step and the inside part of the Pyrex wall is smaller than the total height H of the channel, which is smaller than the width W of the channel. In the microdiaphragm configuration, the width w of the rectangular diaphragm must be the smallest size in front of the height H of the channel and the width W of the channel. We note indistinctively l the length of the diaphragm or the length of the top of the step, for MDD and MSD respectively. L is the total length of the channel. A snapshot of a micro step device (MSD) is presented in Figure 1-a. The characteristic sizes of the devices under test are presented in table 1. For both devices the inception of cavitation is expected to arise for a pressure drop $\Delta P \approx 5$ bars. The main difference between the two kinds of devices is the respective flow rate ; the MSD geometry is applicable with large channels, that makes possible hydrodynamic cavitation 'on a chip' with relatively large flow rates (≈ several liters/hour). As a consequence of the smallest flow area of the MDD geometry, the maximum flow rate of microdiaphragms devices is around 1 liter / hour when $\Delta P \approx 10$ bars.

	H (µm)	W (µm)	L (cm)	l (µm)	w (µm)	h (µm)
MSD	377	806	4	1	-	125
MDD	165	520	4	58	101	-

Table 1. Geometrical sizes of the two microchannels under test.

The set up devoted to the hydraulic connections and to the liquid supply has been described elsewhere [28, 35]. We recall that the liquid under test is initially poured inside a butyl membrane located inside a tank (Figure 1-b). Degassing is performed by pumping down to ≈ 25 mbar during 10 minutes the air volume located onto the liquid, inside the membrane, (Figure 1-b valves V_1, V_2 V_3 open, the other valves being closed). Then, the open valves are closed and the tank is let at rest during 16 hours, in order to reach a thermodynamic equilibrium that must prevent from concentration gradient in the liquid. The low pressure vapour phase, which is present upon the liquid, is expelled from the flexible membrane by gently opening valves V_2 and V_4. As soon as some liquid emerges at V_2 level, this valve is closed. Concerning experiments performed with air saturated water, the air, which is initially present upon the liquid inside the flexible membrane, was also expelled in the same way. In that case, a slight overpressurization was exerted to the membrane to push the air away. In order to drive the liquid through the microdevices, a pressurized gas is filled inside the tank in order to exert a mechanical force onto the external side of the flexible butyl membrane. That procedure prevents from unintented air engassing. A microphone (RS780-0734) is glued onto the mechanical support of the channel, in order to record the inception of cavitation. A Hamamatsu H10722-110 PMT, whose sensitive cell has a diameter Ø = 8 mm, is mounted in

a 3D translation stage and located in front of the transparent part of the channel, the cell being at a distance d from the top of the Pyrex cap. The cathod radiant sensitivity is announced to be 110 mA/W at 400 nm, so that the quantum efficiency of the PMT is 34.2 %. The amplified signal from the PMT (gain : 10^6) is recorded by a Lecroy wavesurfer 62Xs. A scheme of the experimental set up with detection systems is depicted in Figure 1-b. The liquid passes through a filter made up of two stainless steel grids with a mesh size of 40 µm, located upstream the microreactor. It is collected in a beaker downstream and the dissolved O_2 concentration (ppm correspond here to mg/L) is measured with an Orion 3 star oxymeter. With the procedure described above, we obtain degassed solutions with dissolved O_2 concentrations around 4 ppm. When working with alkaline solutions of luminol as the working fluid, the pH value is also recorded. A light – tight box is put onto the area including the microreactor and the PMT. A flexible foam gasket between the base of the box and the table supporting the experiment ensures an excellent prevention against undesirable external photons. The few holes allowing electronic and hydraulic connections are carefully clogged with modeling clay.

The alkaline solutions of luminol were prepared from luminol (3 – aminophthalhydrazide 97%) powder purchased from Sigma – Aldrich. 170 mg of luminol powder was dissolved in 15 ml of 3.75 mM NaOH solution that was diluted with 1 L of DI water to achieve a solution with pH = 11.73.

A signal processing is needed to get a quantitative analysis of the number of photons that might be emitted. We are expecting for random events, that are not subject to produce a DC voltage but rather a series of discrete pulses [18]. One must be able to discriminate between the electronic noise of the PMT and the luminescent signal, and to record the signal over a duration providing a convergence of the rate of events, for a fixed flowrate. A MATLAB code has been developped, tested, and validated with periodic referenced signals (square waves at 100 Hz and 1 kHz) at different sampling rates (50 kHz, 5 MHz and 50 MHz). The code provides the right values of the frequencies and of the area of the recorded voltage integrated over time. During the experiments, series of signals were recorded during 10 seconds and sampled at a rate of 2.5 Mpoints/sec. Sampling of the 10 seconds long signals has experimentally lead to converging and repeatable results, within ± 2%. The code counts a number of events once the voltage rises above a threshold level. The sensitivity of the counting is limited by the frequency bandwidth of the PMT, from DC to 20 kHz. During the decay time of each peak, when the signal is still above the threshold value, no supplemental event can be recorded. The number of peaks crossing above a threshold value includes both the physical events caused by the photons but also the possible tribute of the electronic noise of the PMT. Due to the noise, a too low threshold value will display a diverging number of events, that has no correlation with luminescent phenomena inside the flow. A too high threshold value will miss most of the events. The curve of the recorded number of events per second plotted as a function of the threshold voltage is decreasing, but it displays a break when the contribution due to the noise is vanishing. For different flow rate conditions and with the PMT gain value of 10^6, that break has always occured for a threshold value of 0.02 V, which was thus the fixed threshold value used for all the experiments presented here.

Considering the small volumes associated to hydrodynamic cavitation 'on a chip', it is realist to expect that light, if any, is emitted spherically outward from a point source (figure 1-b). The cell of the PMT will capture only a part α of the photons, that formulate :

$$\alpha = \frac{1}{2}\left[1 - \frac{x}{(1+x^2)^{1/2}}\right] \qquad (1)$$

with x = 2d/Ø. To cancel the effect of the distance d on the measurement, it is then possible to calculate a total number of events by dividing the recorded number of events by α. Hence, one does not take into account the rate of photons that are reflected from the bottom silicon side of the channel.

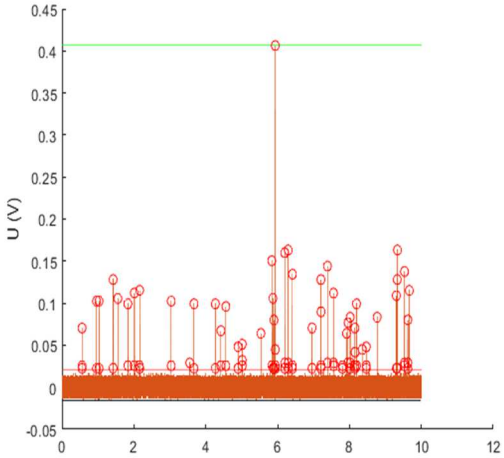

a) ΔP = 0 bar

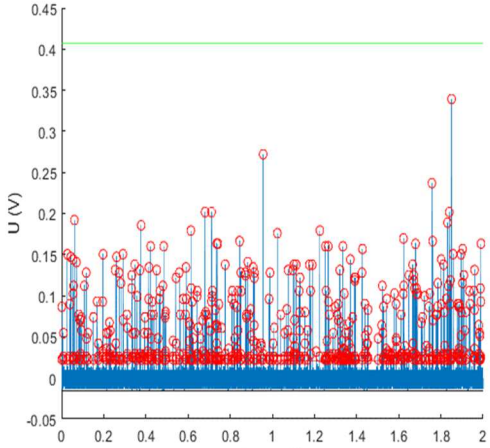

b) ΔP = 5 bars (water)

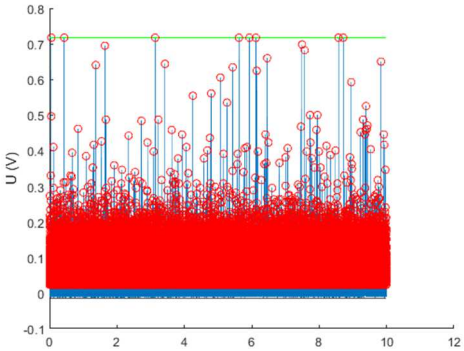

c) ΔP = 5 bars (luminol)

Figure 2. *Screenshot of the LeCroy oscilloscope displaying the detection of photons emitted from the microstep device. a) Single phase water liquid flow ; b) Two-phase cavitating water flows (ΔP = 5 bars) ; c) Two-phase cavitating alkaline luminol solution flow (ΔP = 5 bars). The gap between the top of the microchannel and the cell of the PMT is d = 10 mm .*

3. Results and discussion

Experiments were performed at ambient temperature. The hydrodynamic characterizations of the microdevices MSD and MDD have been first measured with deionized water as the working fluid. The total pressure drop is mainly monitored by the constriction inside the channel, and obeys :

$$\Delta P = K.\ ½.\rho u^2 \qquad (2)$$

where ρ is the density of water (ρ = 1000 kg/m^3), u is the average velocity (m/s) through the constriction. One finds experimentally K = 1.67 and K = 1.76 for the microstep and the microdiaphragm devices respectively. For MSD, the inception of cavitation arises above the critical flow rate Q_{cav} = 3.1 ml/s, corresponding to u = 24 m/s and ΔP = 5 bars. For MDD, the

inception of cavitation arises above Q_{cav} = 0.5 ml/s, corresponding to u = 28 m/s and ΔP = 7 bars.

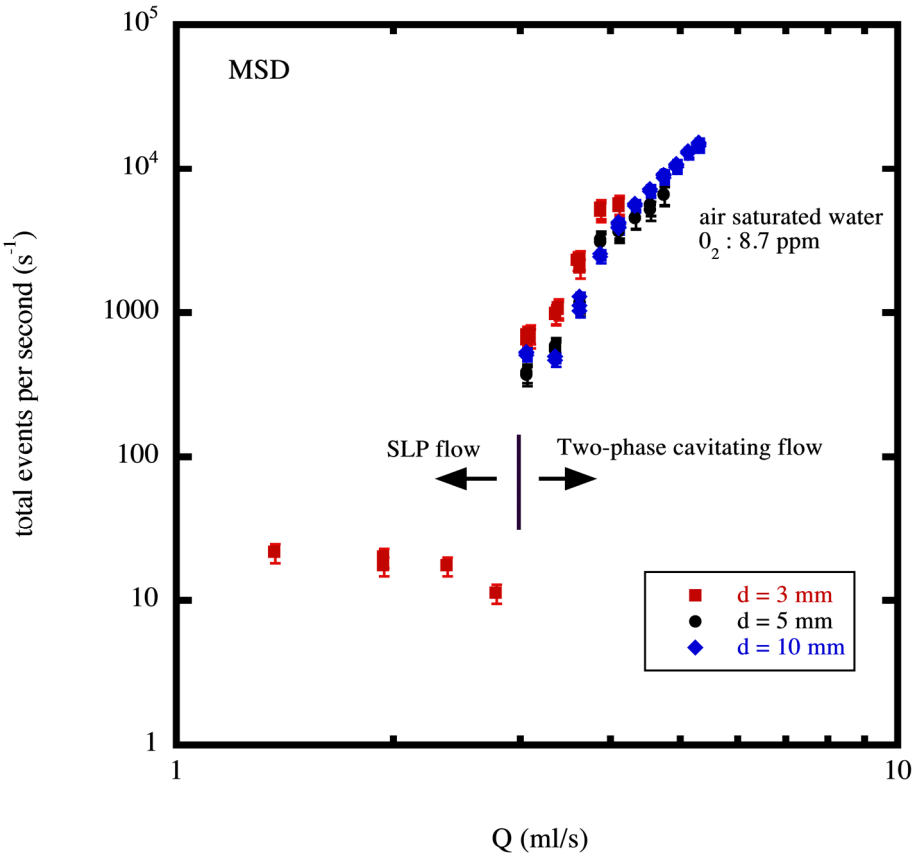

Figure 3. *Total rate of luminescent photons as a function of the flow rate through the microstep device. SLP : single liquid phase. Experiments have been performed for three different values of the gap d.*

With air saturated deionized water as the working fluid, luminescence was detected from the microstep device MSD as soon as a cavitating two-phase flow regime has been reached (Figure 2-b). These experiments have been performed at three different working distances d = 3 mm, 5 mm and 10 mm. The number of recorded events decreased when increasing the gap d. The uncertainty on d (± 0.5 mm) gives way to a relative uncertainty ± 15% (for d = 3 mm and d = 5 mm) and ± 8% (for d = 10 mm) on the total number of events calculated from eq. (1). The data are displayed in Figure 3. The number of events raises as a power function of the flow rate Q^m with 5 < m < 6. The influence of the nature of dissolved gases has also been confirmed (Figure 4). Experiments performed with degassed water (O_2 = 3.8 ppm) have displayed a stronger light emission rate than experiments performed with air saturated water (O_2 = 8 ppm). That is consistent with the assumption that polyatomic molecules present inside a bubble are likely to quench the intensity of the collapse. Degassed water harbours dissolved argon gas in a fewer extend, but the molecules of that monoatomic noble gas are then more likely to be ionized. Moreover, we have also noticed the role of monoatomic rare gases as

being the cause of luminescence in hydrodynamic cavitation 'on a chip'. Deionized water was submitted to a pure argon (respectively xenon) atmosphere at 1 bar during 5 hours. These mixtures were then immediatly passed through the device, with $\Delta P = 5$ bars (that is just above the critical pressure drop of the inception of cavitation for that device). In that particular condition, the photons rate is one and two orders of magnitude (for argon and xenon respectively) greater than with air saturated water.

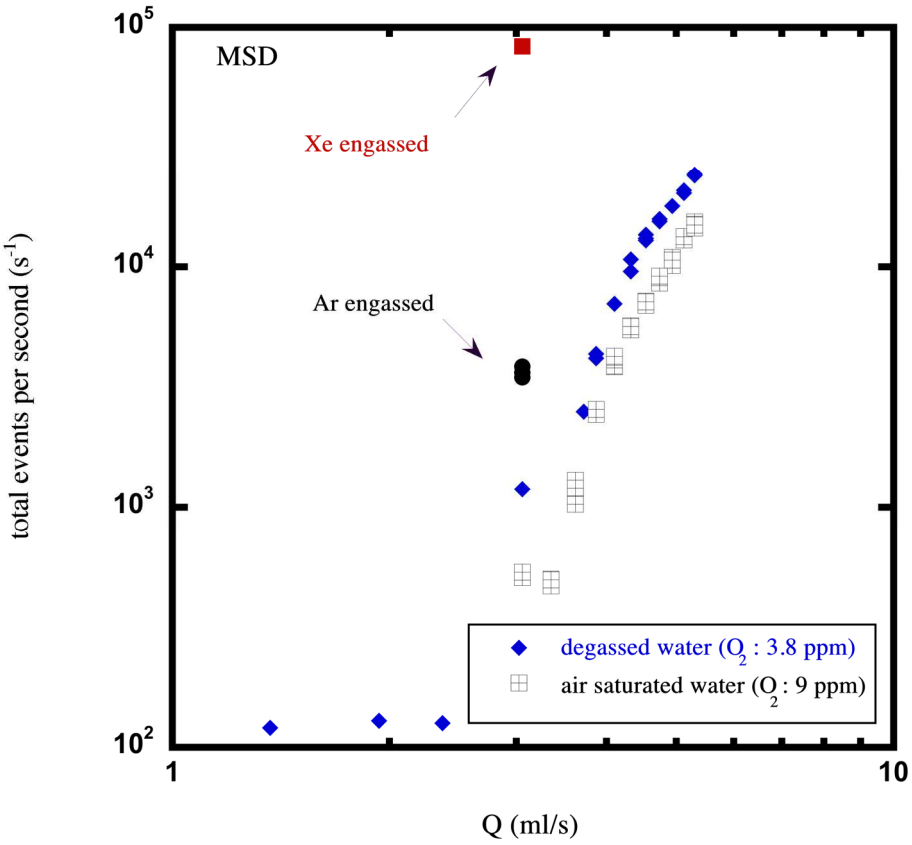

Figure 4. *Total rate of luminescent photons as a function of the flow rate through the microstep device for air saturated water and degassed water. Data recorded with argon and xenon engassed water are also presented. Experiments have been performed with d = 10 mm.*

Chemiluminescence of luminol solutions flowing through the microstep device MSD has been characterized as a function of pH, of the distance between the PMT and the device, and of the role of the dissolved gases.

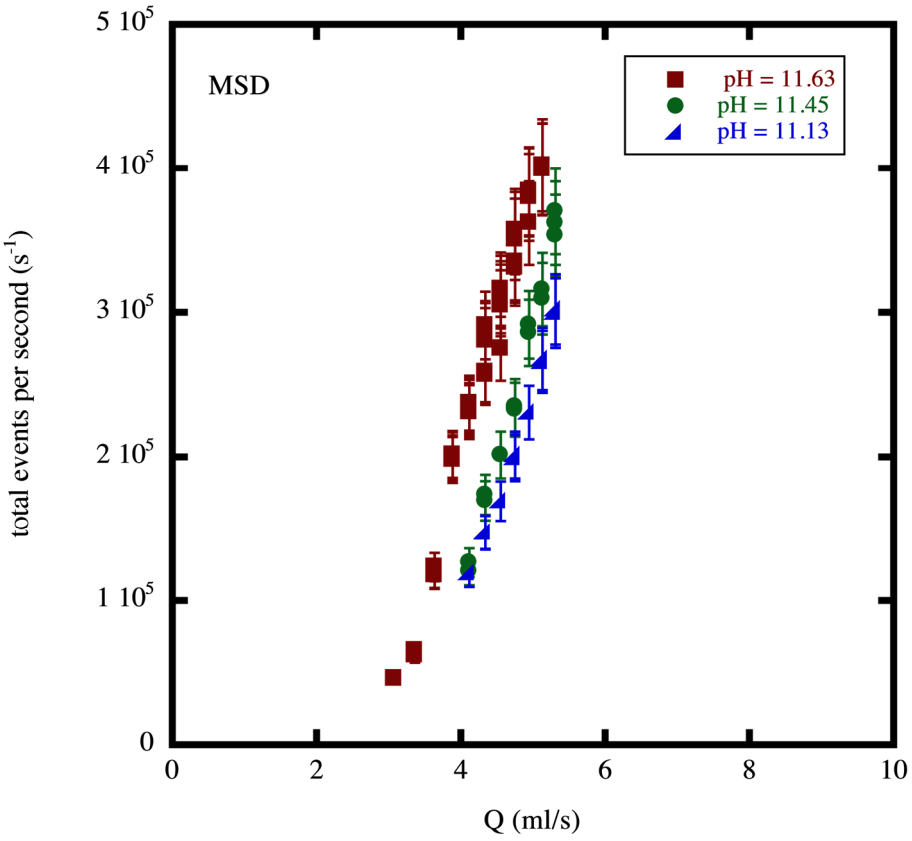

Figure 5. *Total rate of photons emitted from cavitating luminol solutions at different pH values, plotted as a function of the flow rate through the microstep device.*

The number of events recorded without any flow or in the single liquid phase flow was one order of magnitude higher than what was recorded in the same conditions with pure deionized water. That difference cannot be the consequence of external photons having entered inside the black box, nor the consequence of the fluorescence of luminol that they could induce. It is possible that such a signal could be induced by reactions between luminol and some contaminants issue from the hydraulic device [36]. Whatever, such a residual signal is negligible in front of the chemiluminescent intensity recorded as soon as hydrodynamic cavitation arises (Figure 2c). For similar values of pH of the solution under test, the signal logically decreases when the gap d increases, and a calculation of a total number of events, funded on eq. (1), is also possible. As for acoustic cavitation [5, 37], chemiluminescence is strongly dependent on the pH value of the luminol solution (Figures 5, 6). For example, at the maximum tested flow rate of 5 mL/s corresponding to a strong cavitating flow with ΔP = 13 bars, the number of recorded events is nearly halved from pH = 11.63 to pH = 11.13. The chemiluminescence quantum yield of luminol is dependent on pH and on oxidizing conditions [38]. Mc Murray and Wilson [5] highlighted the analogy between cavitation and radiolysis, regarding the production of radical species in water. Chemiluminescence of luminol had been used to detect low concentrations of radical species created in water by radiolysis [7-9]. These studies have concluded that the luminescence requires the participation of both $OH^{\bullet}$ and O_2^{-}

radicals, the reactivity of the later being pH dependent. The intensity of the chemiluminescence is monitored by the radical ($OH^{\bullet}$ or O_2^-) the fewest in number [9].

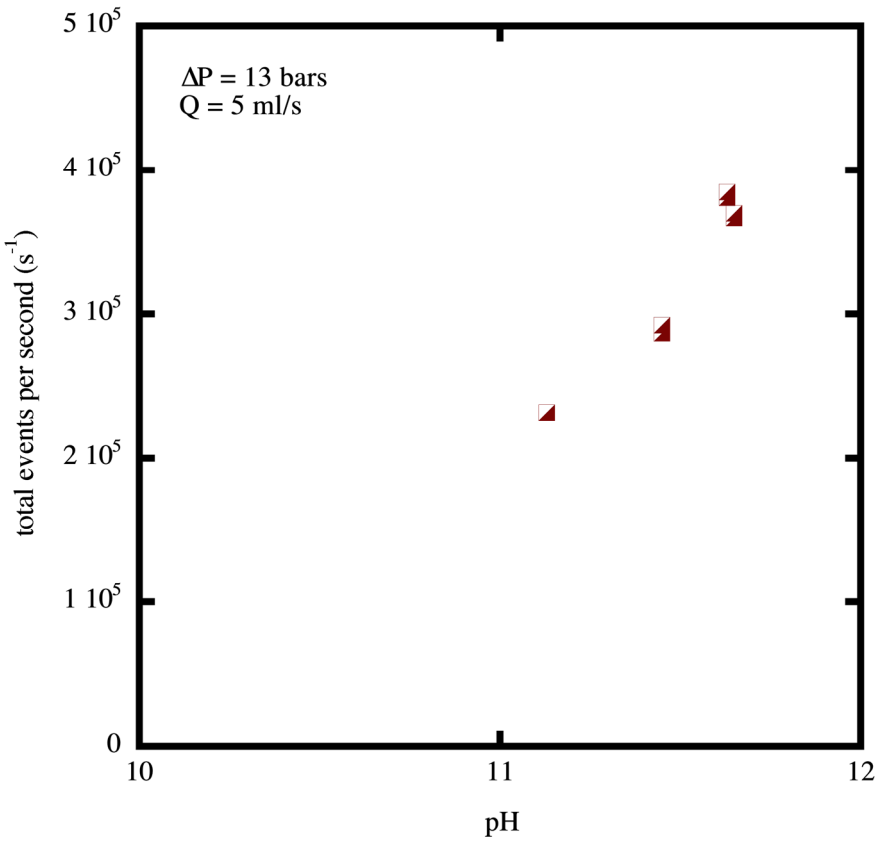

Figure 6. *Dependance of the hydrocavitating chemiluminescence of luminol as a function of the pH value. Data were recorded with the microstep device.*

We have observed that the chemiluminescence of degassed luminol solutions was stronger than the chemiluminescence of air saturated solutions (figure 7). At a fixed flow rate, the difference between the number of events emitted by degassed and undegassed cavitating luminol solution is greater than the contribution expected from the single luminescence phenomena. However, it has been claimed that O_2 promotes $OH^{\bullet}$ radicals and H_2O_2 formation [6, 39]. Otherwise, hydroxyl radicals yield has been measured by potassium iodide dosimetry, and above 20 kHz the presence of dissolved O_2 enhances the yield of that reaction [40]. And the presence of superanion radicals O_2^- is necessary for the chemiluminescence of luminol. The fact that we observe an increase of the number of photons when the concentration of oxygen molecules has been divided by two, is the demonstration that the production of reactive oxygen species, or their diffusion toward the liquid phase, is enhanced when the rate of polyatomic molecules inside the collapsing bubbles has been diminished. Whatever the dissolved gas rate is, a linear evolution of the number of events with the cavitating flow rate is emerging once the cavitating flow has been established (Figure 7).
Additional measurements have been performed with the microdiaphragm device MDD, with air saturated deionized water and luminol solutions as the working fluids respectively, and at

d = 10 mm. Luminescence from deionized water occurs as soon as the cavitating flow regime is activated (Figure 8). Similarly, the chemiluminescence of the luminol solution cavitating through the microdiaphragm device MDD is clearly noticeable, the number of events being sixty times that of luminescence of DI water.

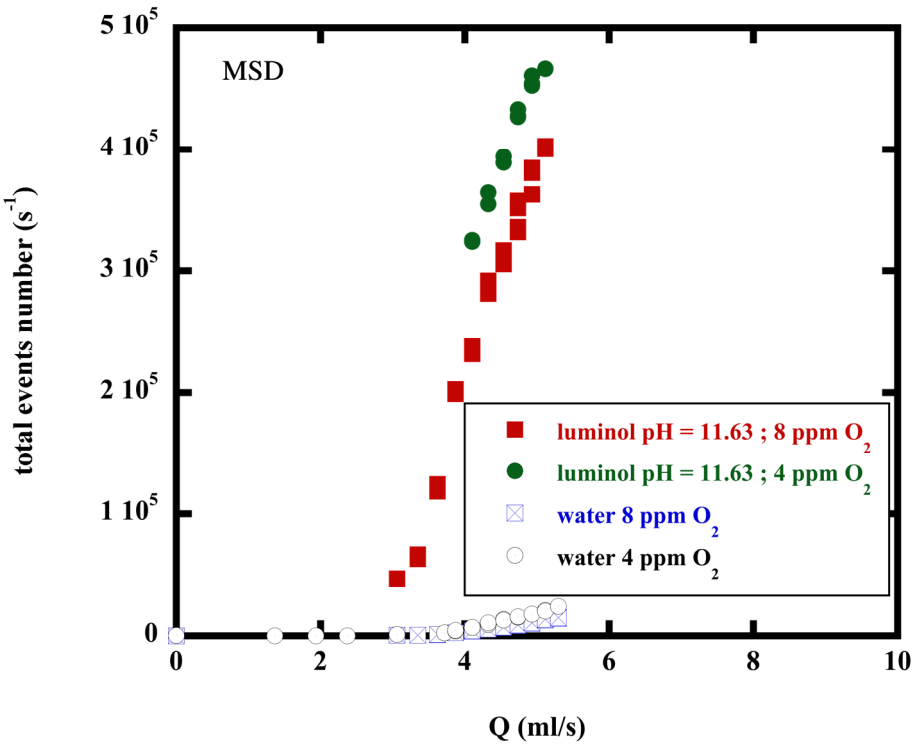

Figure 7. *Compilation of chemiluminescence and luminescence phenomena recorded from the microstep device, for air saturated and degassed luminol and water solutions.*

It is possible to conduct a comparative study between hydrochemiluminescence of alkaline luminol solutions and hydroluminescence of water, because corresponding data were recorded under similar cavitating flow regimes. Data from both devices under test have been gathered and plotted in Figure 9, as a function of the relative flow rate Q/Q_{cav}. The evolution of the ratio CL/L between the number of photons emitted by chemiluminescence (CL) and the number of photons emitted by luminescence (L) does not depend on the uncertainties on backscattered photons, quantum efficiency of the PMT and of the chemiluminescence of luminol. The number of radicals involved in the chemiluminescent reactions is higher than the number of purely luminescent photons, that was expected because it is already happening for single bubble sonoluminescence with spherical collapse [41]. Concerning the microstep device, the ratio CL/L is high and decreases quickly when increasing the flowrate. That is the consequence of the strong increase of the hydroluminescent events that occurs just above the inception of cavitation. Such an evolution is not observed with the microdiaphragm device, for which the ratio CL/L is constant. That illustrates the role of the total pressure drop on the hydroluminescence. The pressure exerted on a collapsing bubble downstream the diaphragm or the microstep depends on the total exerted pressure drop ΔP. The inception of cavitation occurs at ΔP = 5 bars for MSD but at ΔP = 7 bars for MDD, that must be strong enough so that spherical collapsing bubbles may emit light. As a matter of fact, the rise of

hydroluminescence for MSD lessens when $\Delta P > 8$ bars corresponding to $Q/Q_{cav} > 1.3$. (Figures 3, 9). The ratio CL/L is found to be the highest when working with air engassed solutions. When working with degassed solutions, the relative increase of chemiluminescent events is lower than the relative increase of hydroluminescent events, even if the absolute variation of CL events is still predominent (Figure 7).

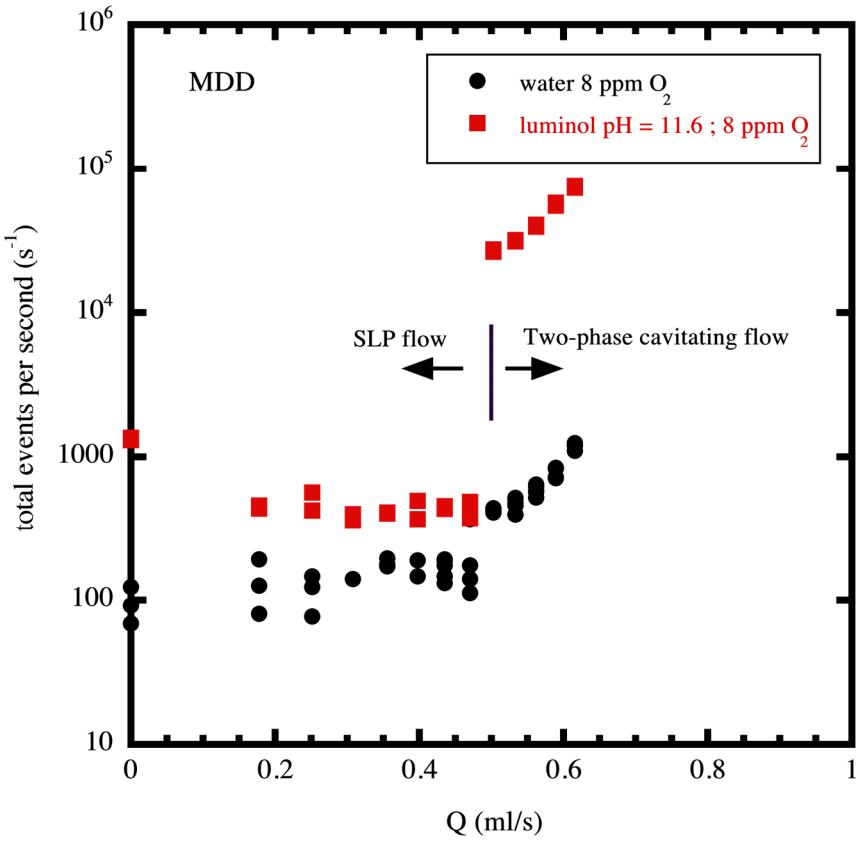

Figure 8. *Total rate of photons emitted by luminescence and chemiluminescence from the microdiaphragm device. SLP : single liquid phase.*

A minimum global estimation of the quantitative number of hydroxyl radicals produced by the collapse of the bubbles is reachable even though it results from rough calculations. Assuming that one recorded event is the signature of one single photon, the estimation of the hydroxyl radicals yield faces some unknown parameters. First, as both $OH^{\bullet}$ and O_2^- radicals are required for chemiluminescent emission from luminol, the number of photons is monitored by the specy the lowest in number. When $OH^{\bullet}$ radicals are less present than O_2^- radicals, the chemiluminescent signal of luminol act as a dosimeter of $OH^{\bullet}$ radicals. But when $OH^{\bullet}$ radicals are in excess against O_2^- radicals, one can only get a lower bound of the number of $OH^{\bullet}$ radicals, as no more light is emitted when the superoxide anions O_2^- have been consumed. Other limitations are caused by the experimental set up by itself. The optical transmittance of the Pyrex© cap is 90 % for the wavelengths recorded by the PMT. The calculation, from eq. (1), of the total number of emitted photons may be two-fold overrated by photons that are backscattered from the bottom of the channel. The quantum efficiency of the

PMT is precisely known only for photons whose wavelength is 400 nm. The quantum chemiluminescent yield of luminol reactions, which is much lower than its fluorescent efficiency, depends strongly on oxidizing conditions [38]. Moreover, $OH^{\bullet}$ radicals will react with luminol but they can also dimerize to H_2O_2. We employ here a chemiluminescence quantum yield Q_C = 0.0124 determined in aqueous solutions [38]. So, from the hypothesis listed above, we calculate that one total event corresponds to 262 reacting radicals. We can express an apparent hydroxyl radicals rate per liter or per unit of hydraulic energy. Results are presented in table 2. For the microchannel MSD used with degassed luminol solutions, we have recorded 4.67×10^5 photons/sec at Q = 5.1ml/sec with ΔP = 14 bars (4×10^5 photon per second with air engassed luminol solutions under the same hydraulic conditions). For the microchannel MDD we only tested air engassed luminol solutions, and we got 75×10^3 photons/sec at Q = 0.62 ml/sec with ΔP = 12 bars. The single hydroluminescence rates are also listed in table 2. They have been calculated from 24300 photons/sec recorded at Q = 5.3 ml/sec with ΔP = 15 bars for degassed water flowing through MSD (15000 photons/sec for air engassed water) ; and from 1200 photons/sec recorded at Q = 0.60 ml/sec with ΔP = 12 bars for air engassed water flowing through the microchannel MDD.

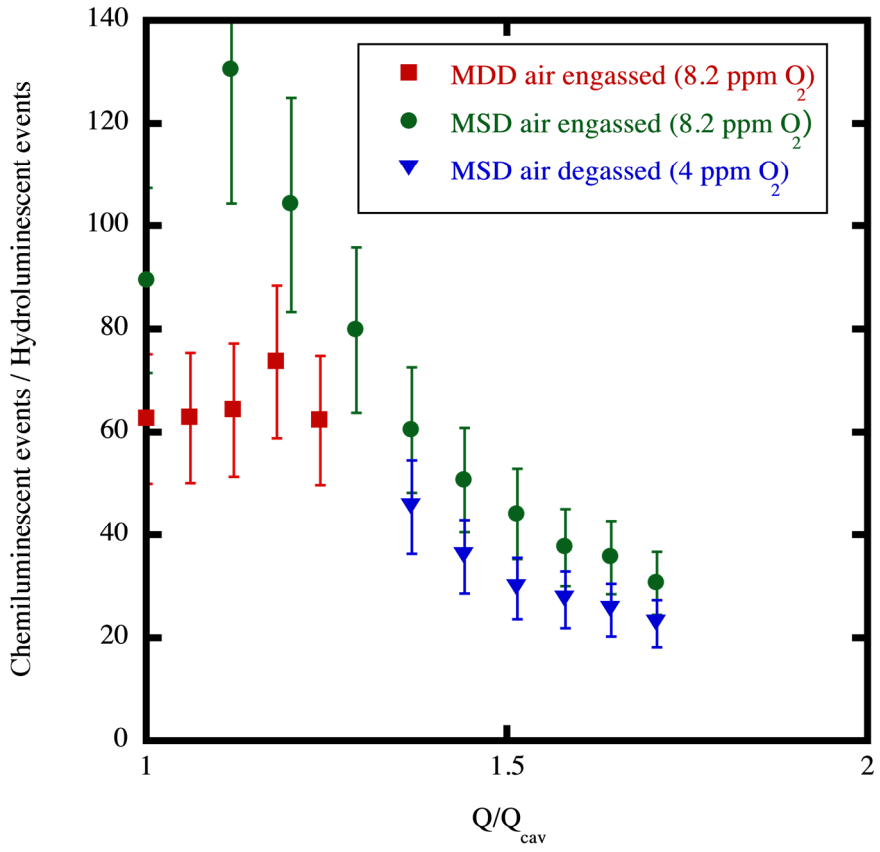

Figure 9. *Chemiluminescent events divided by luminescent events, as a function of a reduced flow rate.*

	Chemiluminescence		Hydroluminescence	
	$OH^{\bullet}$/L	$OH^{\bullet}$/J	photons/L	photons/J
MSD degassed	$2.4\ 10^{10}$	$17\ 10^{6}$	$14.9\ 10^{6}$	9930
MSD air saturated	$2.1\ 10^{10}$	$15\ 10^{6}$	$9.2\ 10^{6}$	6130
MDD air saturated	$3.3\ 10^{10}$	$26\ 10^{6}$	$6.5\ 10^{6}$	5400

Table 2. Rates of $OH^{\bullet}$ radicals and photons reduced to the unit of volume and hydraulic energy.

These results confirm previous results obtained for chemiluminescence with devices similar to MDD, and for which we got $1.6\ 10^{10}$ $OH^{\bullet}$/L and $15\ 10^{6}$ $OH^{\bullet}$/J [28]. These whole results have been recorded at flow regimes for which $Q/Q_{cav} < 2$, that means that cavitation was not fully developped. By considering in figures 7 and 8 the slope of the curve above Q_{cav}, one finds a dynamic evolution around 10^{11} $OH^{\bullet}$/L for both devices. Concerning the radicals production, there is no obvious difference between the efficiency of each sort of devices. As the two profiles develop shear cavitation, similar bubbles dynamics are expected. From table 2, one can hardly notice a slight enhancement of hydroluminescence for MSD design and a slight enhancement of chemiluminescence for the MDD design, but complemental results from MDD with degassed fluids should be required to draw a firm conclusion.
The estimated rate of hydroxyl radicals measured in our microchannels is six orders of magnitude lower than the rate published by Arrojo et al [42] for hydrodynamic cavitating flows in a macrosized device. The authors used hydrophobic salicylic acid solutions as $OH^{\bullet}$ scavenger, and the flow was driven by a pump in which cavitation could also occur [25]. The pressure drop and the average velocity of the fluid had similar values as ours. No evidence can be found that the lower rate we find is only due to an easier recombination of most of the $OH^{\bullet}$ radicals, before they could react with luminol molecules. The scale of the cavitating devices used in macroscopic and microscopic experiments may explain the mismatch between the results of Arrojo et al [42] and ours. This can also be related to the fact that the experiment has counted a number of O_2^- radicals, which were fewer in number than $OH^{\bullet}$ radicals. Whatever is the flow rate, the size of the vapour pocket downstream the constriction must be a key parameter, as being at the origin of the number of shedded collapsing bubbles. For devices passed by fluids driven at similar velocities, the ratio of the respective flow rates is the ratio of the cross sections of the respective constrictions. But the length of the vapour pocket downstream depends on the output pressure of the device. The lack of details on the hydrodynamic characteristics of the experiments of Arrojo et al [42] does not permit to acceed that parameter and to compare it to our observations. In steady state flows conditions, the collapse of bubbles is balanced by vaporisation of liquid phase. Thermodynamics of liquid – vapour transition should be considered in the analysis of the yield of $OH^{\bullet}$ production. At least, the lifetime of bubbles is a parameter that may define a pseudo frequency for hydrodynamic cavitation, comparable to that used in acoustic cavitation. However, it is obvious that the 'one-shot' collapse in hydrodynamic cavitation does not obey exactly to the same physics as a multiperiodically monitored acoustic bubble. It is known that hydrodynamic cavitation at macroscale induces pseudo low frequencies, and that was argued as a cause of the low efficiency of the process for hydroxyl radicals production [7, 42]. Optical observations of the two phase cavitating flow through the microdevices MSD and MDD have demonstrated that the average path of collapsing bubbles is globally between 150 µm and 500 µm. Considering that these bubbles are drawn by the emerging liquid jet at a velocity ≈ 30 m/s, one may assign to lifetimes, which lie between 5 µs and 15 µs, a pseudo frequency range between 33 kHz and 100 kHz. That match the optimum frequencies used in chemical sonoreactors [7, 43]. From

that point of view, the production of hydroxyl radicals in hydrodynamic cavitating reactors should be enhanced by the small size of the device.

4. Conclusion

A quantitative evaluation of the number of hydroxyl radicals and photons created in hydrodynamic cavitating flows has been performed inside dedicated microsystems. The luminescence is caused by incondensable noble gases present inside the collapsing bubbles, and air degassed solutions logically enhance the luminescence by lowering quenching during the collapse. The level of luminescence is monitored by the pressure exerted upstream. The hydroxyl radical production has been estimated from the chemiluminescence of luminol. Air degassed luminol aqueous solutions have proven to enhance the formation of reactive oxygen species, but to a lower extend than degassed water enhances the luminescence. The maximum calculated rate of $OH^{\bullet}$ radicals was around 10^{-12} mol/L, that is a lower bound because the whole hydroxyl radicals did not participate for sure to the chemiluminescence. The volume of the vapour phase in the cavitating flow regime, and the rate of mass transfer between liquid and vapour phase, are parameters that will be considered for possible enhancements of light and chemical emmissions. Further works should monitor acoustic cavitation inside these microchannels, where larger luminescent and chemiluminescent emissions should be expected.

Acknowledgments

The author acknowledge the financial support from the Centre National de la Recherche Scientifique (C.N.R.S.) via the program ‘green engineering’ of the INSIS Department. They also acknowledge the TEC XXI fundation which has provided the post doctoral fellowship of one of us (L.P.). Deep reactive ion etching was kindly performed by A. Barbier and Dr E. Griessen at IRAM, Grenoble. Other micromachining steps were performed thanks to the Nanofab facilities at the Neel Institute of Grenoble. Helpful technical assistance was furnished by V. Govart from LEGI. The authors acknowledge Dr G. Ledoux for useful discussions.

L.P. built the experimental set up, developed the Matlab code, performed the experiments, analysed the data.
D.C. has micromachined the samples and designed the hydraulic circuitry, developed the Matlab code, contributed to the implementation of the experimental set up.
F.A. initiated the work, participated to the implementation of the experimental set up, analysed the data and wrote the paper.

References

[1] D.J. Flannigan, K.S. Suslick, Plasma formation and temperature measurement during single-bubble cavitation, Nature 434 (2005) 52-55.
[2] K.S. Suslick, N.C. Eddingsaas, D.J. Flannigan, S.D. Hopkins, and H. Xu, The chemical history of a bubble, Acc. Chem. Res. 51 (2018), 2169-2178.
[3] K.J. Taylor, P.D. Jarman, Spectrum and lifetime of the acoustically and chemically induced emission of light from luminol, J. Am. Chem. Soc. 93 (1971) 257-258.
[4] V. Renaudin, N. Gondrexon, P. Boldo, C. Pétrier, A. Bernis and Y. Gonthier, Method for determining the chemically active zones in a high-frequency ultrasonic reactor, Ultrason. Sonochem. 1 (1994) 81-85.
[5] H.N. McMurray and B.P. Wilson, Mechanistic and spatial study of ultrasonically induced luminol chemiluminescence, J. Phys. Chem. A 103 (1999) 3955-3962.

[6] S. Hatanaka, H. Mitome, K. Yasui and S. Hayashi, Single-bubble sonochemiluminescence in aqueous luminol solutions, J. Am. Chem. Soc. 124 (2002) 10250-10251.
[7] J.H. Baxendale, Pulse radiolysis study of the chemiluminescence from luminol, Trans. Faraday Soc. 69 (1973) 1665-1677.
[8] E. Würzberg and Y. Haas, A pulse radiolysis study of the chemiluminescence of some luminol-like molecules, J. Phys. Chem. 83 (1979) 2687-2692.
[9] V. Wasselin-Trupin, G. Baldacchino, S. Bouffard, E. Balanzat, M. Gardès-Albert, Z. Abedinzadeh, D. Jore, S. Deycard, and B. Hickel, A new method for the measurement of low concentrations of OH/O2- radical species in water by high-LET pulse radiolysis. A time-resolved chemiluminescence study, J. Phys. Chem. A 104 (2000) 8709-8714.
[10] S. Arrojo, Y. Benito, A theoretical study of hydrodynamic cavitation, Ultrason. Sonochem. 15 (2008) 203-211.
[11] B.D. Storey and A.J. Szeri, Water vapour, sonoluminescence and sonochemistry, Proc. R. Soc. Lond. A 456 (2000) 1685-1709.
[12] P.D. Jarman and K.J. Taylor, Light emission from cavitating water, Brit. J. Appl. Phys. 15 (1964) 321-322.
[13] P.D. Jarman and K.J. Taylor, Light flashes and shocks from a cavitating flow, Brit. J. Appl. Phys 16 (1965) 675-683.
[14] Y.T. Didenko, W.B. McNamara III, and K.S. Suslick, Temperature of multibubble sonoluminescence in water, J. Phys. Chem. A 103 (1999) 10783-10788.
[15] F.B. Peterson and T.P. Anderson, Light emission from hydrodynamic cavitation, Phys. Fluids 10 (1967) 874-879.
[16] K.R. Weninger, C.G. Camara, and S.J. Putterman, Energy focusing in a converging fluid flow : implications for sonoluminescence, Phys. Rev. Lett. 83 (1999) 2081-2084.
[17] T.G. Leighton, M. Farhat, J.E. Field and F. Avellan, Cavitation luminescence from flow over a hydrofoil in a cavitating tunnel, J. Fluid Mech. 480 (2003) 43-60.
[18] M. Farhat, A. Chakravarty and J.E. Field, Luminescence from hydrodynamic cavitation, Proc. R. Soc. A 467 (2010) 591-606.
[19] C. Whitfield, M. Foulkes, and E. Hywel Evans, Cavitating flow luminescence as a potential source for analytical spectroscopy, Materials Performance and Characterization 7 (2018) 1004-1017.
[20] D.A. Biryukov, D.N. Gerasimov, Spectroscopic diagnostics of hydrodynamic luminescence, J. Mol. Liq. 266 (2018) 75-81.
[21] K.S. Suslick, M.M. Mdleleni, and J.T. Ries, Chemistry induced by hydrodynamic cavitation, J. Am. Chem. Soc. 119 (1997) 9303-9304.
[22] K.M. Kalumuck, G.L. Chahine, The use of cavitating jets to oxidize organic compounds in water, J. Fluids Eng. 122 (2000) 465-470.
[23] A.G. Chakinala, P.R. Gogate, A.E. Burgess, D.H. Bremner, Industrial wastewater treatment using hydrodynamic cavitation and heterogeneous advanced Fenton processing, Chem. Eng. J. 152 (2009) 498-502.
[24] P. Braeutigam, Z.-L. Wu, A. Stark, B. Ondruschka, Degradation of BTEX in aqueous solution by hydrodynamic cavitation, Chem. Eng. Technol. 32 (2009) 745-753.
[25] P. Braeutingam, M. Franke, Z.L. Wu, B. Ondruschka, Role of different parameters in the optimization of hydrodynamic cavitation, Chem. Eng. Technol. 33 (2010) 932-940
[26] R.D. Lockett, A. Bonifacio, Hydrodynamic luminescence in a model diesel injector return valve, Int. J. Eng Res, 7 (2019)
[27] M. Schlender, K. Minke, H.P. Schuchmann, Sono-chemiluminescence (SCL) in a high-pressure double stage homogenization processes, Chem. Eng. Sci. 142 (2016) 1-11.

[28] D. Podbevsek, D. Colombet, G. Ledoux, F. Ayela, Observation of chemiluminescence induced by hydrodynamic cavitation in microchannels, Ultrason. Sonochem. 43 (2018) 175-183.
[29] Y. Tao, J. Cai, X. Huai, B. Liu, Z. Guo, Application of hydrodynamic cavitation to wastewater treatment, Chem. Eng. Technol. 39 (2016) 1363-1376.
[30] R. Cirimina, L. Albanese, F. Meneguzzo, M. Pagliaro, Wastewater remediation via controlled hydrocavitation, Environ. Rev. 25 (2017) 175-183.
[31] M. Medrano, P.J. Zermatten, C. Pellone, J.P. Franc and F. Ayela, Hydrodynamic cavitation in microsystems. I. Experiments with deionized water and nanofluids, Phys. Fluids 23 (2011) 127103.
[32] M. Medrano, C. Pellone, P.J. Zermatten and F. Ayela, Hydrodynamic cavitation in microsystems. II. Simulations and optical observations, Phys. Fluids 24 (2012) 047101.
[33] F. Ayela, M. Medrano-Munoz, D. Amans, C. Dujardin, T. Brichart, M. Martini, O. Tillement and G. Ledoux, Experimental evidence of temperature gradients in cavitating microflows seeded with thermosensitive nanoprobes, Phys. Rev. E 88 (2013) 043016.
[34] S. Mossaz, D. Colombet, F. Ayela, Hydrodynamic cavitation of binary liquid mixtures in laminar and turbulent flow regimes, Exp. Therm. Fluid Sci. 80 (2017) 337-347.
[35] X. Qiu, W. Cherief, D. Colombet and F. Ayela, A simple process to achieve microchannels geometries able to produce hydrodynamic cavitation, J. Micromech. Microeng. 27 (2017) 047001
[36] S. Xu, F. Chen, M. Deng and Y Sui, Luminol chemiluminescence enhanced by copper nanoclusters and its analytical application, RSC Adv. 4 (2014) 15664.
[37] N. Miyoshi, S. Hatanaka, K. Yasui, H. Mitome and M. Fukuda, Effects of pH and surfactant on the ultrasound –induced chemiluminescence of luminol, Jpn J. Appl. Phys., 40 (2001) 4097- 4100.
[38] J. Lee and H.H. Seliger, Quantum yields of the luminol chemiluminescence reaction in aqueous and aprotic solvents, Photochem. Photobiol. 15 (1972) 227-237.
[39] E.L. Mead, R.G. Sutherland, and R.E. Verrall, The effect of ultrasound on water in the presence of dissolved gases, Can. J. Chem. 54 (1976) 1114-1120.
[40] J. Rooze, E.V. Rebrov, J.C. Schouten, J.T.F. Keurentjes, Dissolved gas and ultrasonic cavitation – A review, Ultrason. Sonochem. 20 (2013) 1-11.
[41] Y.T. Didenko and K.S. Suslick, The energy efficiency of formation of photons, radicals and ions during single-bubble cavitation, Nature 418 (2002) 394-397.
[42] S. Arrojo, C. Nerin, Y. Benito, Application of salicylic acid dosimetry to evaluate hydrodynamic cavitation as an advanced oxidation process, Ultrason. Sonochem. 14 (2007) 343-349.
[43] C. Pétrier, A. Francony, Ultrasonic waste-water treatment : incidence of ultrasonic frequency on the rate of phenol and carbon tetrachloride degradation, Ultrason. Sonochem. 4 (1997) 295-300.